Full Paper Transactions, SMiRT 28
Toronto, Canada, August 10-15, 2025

EVALUATING THE EFFECTS OF GAMMA RADIATION ON THE SEISMIC RESPONSE OF ELASTOMERIC ISOLATION BEARINGS

Ajaykumar D. Patel[1], Dean R. Peterman[2], Evans D. Kitcher[3], Chandrakanth Bolisetti[4], and Andrew S. Whittaker[5]

[1]Ph.D. Candidate, Department of Civil, Structural, and Environmental Engineering, University at Buffalo, Buffalo, NY 14260, USA (apatel48@buffalo.edu)
[2]Distinguished Scientist, Idaho National Laboratory, Idaho Falls, ID 83415, USA (dean.peterman@inl.gov)
[3]Spent Fuel Analyst, Idaho National Laboratory, Idaho Falls, ID 83415, USA (evnas.kitcher@inl.gov)
[4]Senior Scientist, Idaho National Laboratory, Idaho Falls, ID 83415, USA (chandrakanth.bolisetti@inl.gov)
[5]SUNY Distinguished Professor, Department of Civil, Structural, and Environmental Engineering, University at Buffalo, Buffalo, NY 14260, USA (awhittak@buffalo.edu)

ABSTRACT

Some advanced reactor developers are considering the use of seismic isolation and damping devices to protect safety-critical assets from the effects of extreme earthquake shaking. If installed near a reactor vessel without shielding, these devices will be exposed to gamma and neutron radiation, which will affect their mechanical properties and may change their response to earthquake shaking. The United States Department of Energy, through its Nuclear Energy University Program, funded a study to characterize the effects of absorbed gamma dose on the mechanical properties of isolators, damping devices, and fluids. This paper describes the seismic protective devices considered in the project, the gamma irradiator, and presents the results of pre- and post-irradiation testing of low-damping rubber (LDR) and lead-rubber (LR) elastomeric bearings irradiated to cumulative absorbed doses of 25, 100, and 200 kGy. The exposure time required to achieve the target dose was determined using a validated Monte Carlo N-Particle model of the gamma irradiator. Results of the physical testing were mixed, with no change in shear modulus for the larger bearings (Type A) at 200 kGy but a meaningful change in shear modulus for the smaller bearings (Type B) at the same absorbed dose.

1. INTRODUCTION

Seismic isolation and damping devices have been deployed in more than 10,000 structures worldwide, over the past 40 years to mitigate the effect of earthquake shaking on bridges, buildings, and mission-critical infrastructure. Because studies have demonstrated that seismic isolation of nuclear power plants can reduce seismic risk by several orders of magnitude (Lal *et al.*, 2022; Yu *et al.*, 2018), some reactor developers are considering seismic isolation as an integral design feature, to be deployed at either the building level, isolating the entire nuclear structure, or at the component level, isolating individual pieces of the nuclear structure such as reactor vessels and steam generators (Mir *et al.*, 2023). In building isolation, the reinforced concrete basemat will shield the seismic protective devices from the possible damaging effects of gamma and neutron radiation. An alternate application of seismic isolation is to equipment inside a reactor building, wherein the devices may be exposed to gamma and neutron radiation, which may affect their mechanical properties and consequently the response of the isolated equipment to design-basis shaking.

The Department of Energy, as part of its Nuclear Energy University Program, is funding a project at the University at Buffalo (UB) to investigate the effects of gamma radiation on the mechanical behavior of various seismic protective devices. (The effects of neutron irradiation on the mechanical properties of seismic isolators are not addressed in this project, as they require extensive resources, including neutron irradiators and hot cell testing, which are beyond the scope of this study.) In this project, different seismic protective devices and components thereof have been subjected to cumulative absorbed gamma doses of 25, 100, and 200+ kGy using an irradiator at the Idaho National Laboratory (INL). (A cumulative absorbed dose of 200 kGy was established as a *reasonable* maximum value by developers of advanced reactors and experts at INL.) Pre-irradiation seismic tests at UB of each device using a Single Bearing Test Machine (SBTM) established baseline mechanical properties. These tests were then repeated after each dose increment to the devices to characterize changes in their mechanical properties as a function of absorbed gamma dose. Monte Carlo N-Particle (MCNP) analysis is being used to estimate absorbed dose in these devices as a function of exposure time. Post-irradiation experiments of the tested elastomers at INL, utilizing Raman spectroscopy, will identify changes at the molecular level as a function of absorbed gamma dose.

2. SEISMIC PROTECTIVE DEVICES

Seismic protective devices under consideration for application to nuclear power plants in the U.S. are shown in Figure 1. The single friction pendulum (SFP) and triple friction pendulum (TFP) isolators of Figures 1a and 1b are spherical sliding bearings. These bearings consist of hemispherical stainless-steel surfaces and a high-load, low-friction composite bonded to the articulated slider(s), which slides across the spherical surface(s). Figure 1c is a cut-away view of a lead-rubber (LR) elastomeric bearing, which comprises alternating layers of bonded natural rubber and carbon steel shims, with a central lead core. The low damping rubber (LDR) elastomeric bearing is the LR elastomeric bearing minus the lead core. Figure 1d is a coil-spring bearing, constructed from nested coil springs. Figure 1e depicts a three dimensional (3D) viscoelastic damper composed of a cylindrical vessel filled with highly viscous fluid and a piston that is immersed in the fluid. Figure 1f is a photograph of a one-dimensional (1D) fluid viscous damper (FVD).

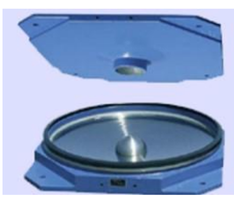

(a) SFP bearing (EPS)

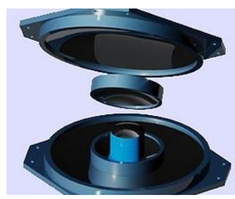

(b) TFP bearing (EPS)

(c) LR bearing (DIS)

(d) coil-spring isolator (GERB)

(e) 3D viscoelastic damper

(f) 1D FVD (Taylor Devices)

Figure 1. Seismic protective devices

At the time of this writing, viscous fluids used in 1D dampers (Patel *et al.*, 2024b), 3D viscoelastic dampers (Patel *et al.*, 2025a), and TFP isolators (Patel *et al.*, 2025b) have been irradiated, and preliminary results on changes in their mechanical properties have been published. This paper presents results of pre- and post-irradiation mechanical testing of the LDR and LR elastomeric bearings.

Two LDR and two LR bearings (176 mm in diameter), denoted Type A (LDR-A1, LDR-A2, and LR-A1 and LR-A2) hereafter, and four LDR bearings (128 mm in diameter), denoted Type B (LDR-B1 to LDR-B4) hereafter, all manufactured by Dynamic Isolation Systems (DIS), were irradiated to cumulative absorbed doses of 25, 100, and 200 kGy. Figure 2 presents the construction drawings of the Type A and Type B LDR and LR bearings. The horizontal force-displacement response of a LDR bearing is essentially linear and proportional to the shear modulus of the elastomer. The horizontal force-displacement response of a LR bearing is bilinear and a function of the diameter and dynamic yield strength of the lead core, the shear modulus and bonded diameter of the elastomer, and the total thickness of the elastomer.

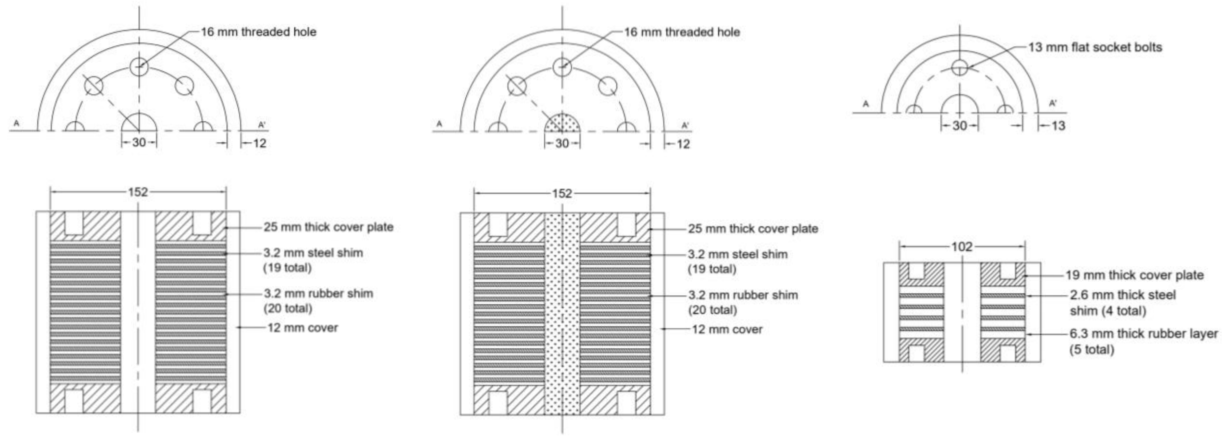

(a) Type A LDR (b) Type A LR (a) Type B LDR

Figure 2. Construction drawings for the LDR and LR bearings (All dimensions are in mm)

3. FTS IRRADIATOR

The Center for Radiation Chemistry Research at INL operates a Foss Therapy Service (FTS) Model 812 gamma irradiator, referred to as the FTS irradiator hereafter. This irradiator, shown in Figure 3a, is a self-contained cobalt-60 gamma irradiator unit. Figures 3b and 3c present a schematic of the FTS irradiator prepared using the MCNP code. Each cobalt-60 (^{60}Co, $\tau_{1/2}$ = 5.27 years, $E_{\gamma 1}$ = 1.17 MeV, and $E_{\gamma 2}$ = 1.33 MeV) source is installed in a nested stainless-steel capsule. The nested capsules are installed in three cylindrical tubes located on one side of the irradiator: two capsules per tube, as shown in Figure 3b. Two of the three tubes, highlighted in Figure 3b, containing a total of four capsules, were active for the irradiation experiments presented in this paper. The body of the FTS irradiator is constructed with layers of lead, highlighted in blue in Figures 3b and 3c. The FTS irradiator includes a turntable to provide a uniform dose to a sample if desired.

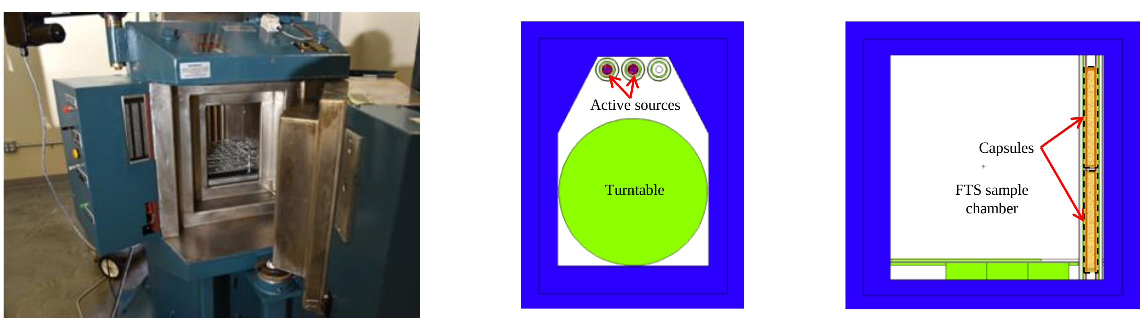

(a) photograph (b) plan (c) cross-section

Figure 3. FTS Model 812 gamma irradiator

4. MCNP MODEL OF FTS IRRADIATOR

Monte Carlo N-Particle of FTS irradiator and its benchmarking

The Monte Carlo N-Particle (MCNP) software is a general-purpose neutron, photon, and charged particle transport code used to simulate particle interaction with matter. It uses the Monte Carlo method and simulates a large number of particle interactions with matter and determines physical quantities, such as energy deposition per unit mass, reaction time, and particle flux in a cell. Patel *et al.* (2025c) developed an MCNP model of the FTS irradiator, shown in Figures 3b and 3c, and validated it using Fricke dosimetry (Fricke *et al.*, 1938), which is a well-established technique for measuring radiation dose.

Approach for achieving target dose to seismic isolators

The MCNP model of the FTS irradiator was used to establish the rate of absorbed dose to the most vulnerable materials (i.e., the elastomer) in the seismic isolators, as described in the next section. The required exposure time to achieve a desired absorbed dose was computed by dividing the target absorbed dose (e.g., 100 kGy) by the MCNP-estimated absorbed dose rate (e.g., 40 Gy/minute): 100 kGy @ 40 Gy/min = 41.6 hours.

5. MCNP MODELS INCLUDING SEISMIC PROTECTIVE DEVICES

Type A LDR and LR bearings

Figure 4 presents cross-sectional views of the MCNP models of the Type A LDR and LR bearings. Each layer of rubber and steel was meshed into 96 cells (6 rings × 16 sectors), each having the same volume. Because the material compositions of the various materials used in bearing construction are proprietary, the atom fractions and material densities required for modeling were adopted from the Pacific Northwest National Laboratory (PNNL) material compendium (Detwiler *et al.*, 2021). The bonded rubber and cover rubber (highlighted in orange in Figure 4) of the bearings are modeled as natural rubber (PNNL material #301) with a density of 0.91 g/cc, and the steel shims (highlighted in red in Figure 4) are modeled as medium carbon steel 1045 (PNNL material #328) with a density of 7.872 g/cc. The modeling details of the various components of the FTS irradiator, such as turntable, source tubes, and source are provided in Patel *et al.* (2024a) and Patel *et al.* (2025c).

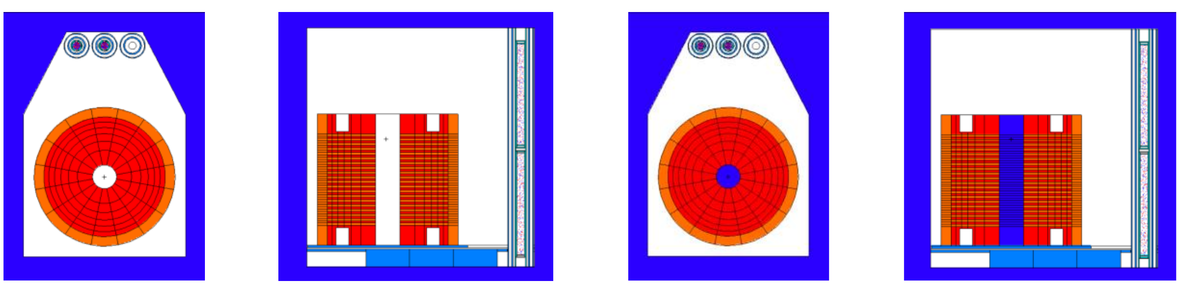

plan | cross-section | plan | cross-section

(a) LDR bearing | (b) LR bearing

Figure 4. MCNP models of the Type A LDR and LR bearings in the irradiator

For the LDR and LR bearings, the middle rubber layer is considered a critical component and so the average absorbed dose rate across all 96 cells of the middle rubber layers was used to calculate the exposure time. The average absorbed dose rates for the LDR and LR bearings, as of January 1, 2024, were 46 and 44 Gy/min, respectively. To calculate the exposure time for a bearing, the absorbed dose rate was then corrected to the irradiation start date for the decay of ^{60}Co ($\tau_{1/2}$ = 5.27 years).

Figures 5b and 5c present the dose rates for the top, middle, and bottom layers of the rubber cells across the diameter (see Figure 5a) of the LDR and LR bearings, respectively, for an *assumed* irradiation date of January 1, 2024. The dose rates for the LDR and LR bearing cells are approximately the same, except for the cells located behind the lead core because it shields gamma radiation, resulting in a 60% average reduction in the dose rates for those cells.

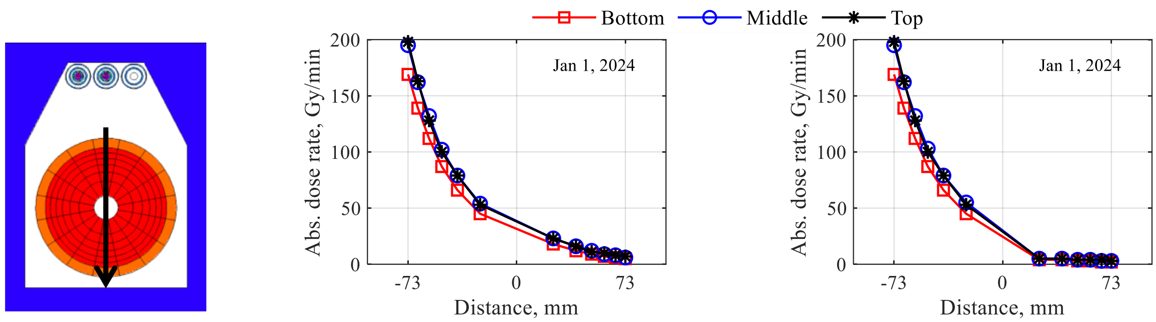

(a) plan (b) LDR bearing (c) LR bearing

Figure 5. MCNP-determined absorbed dose rates for the rubber layers of Type A LDR and LR bearings

Type B LDR bearings

Figures 6a and 6b presents cross-sectional views of the MCNP models of the Type B LDR bearings. The modeling of the Type B LDR bearings is the same as the Type A LDR bearings. The Type B LDR bearings were stacked (see Figure 6b) and irradiated simultaneously. The average absorbed dose rates across all 96 cells of the middle rubber layers of the #1 and #2 bearings, assuming an irradiation start date of January 1, 2024, were 59 and 53 Gy/min, respectively.

Figures 6c and 6d present the dose rates for the top, middle, and bottom layers of the rubber cells across the diameter (see Figure 6a) for bearings #1 and #2, respectively. Like the Type A LDR bearing, the results show an order of magnitude difference in the dose rates between the cell closest to the source and the cell farthest from it. No significant differences are observed in the dose rates among the top, middle, and bottom layers.

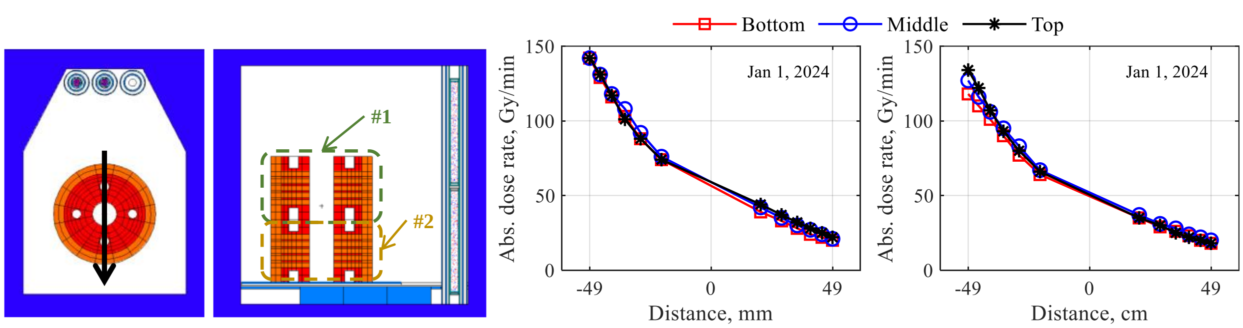

(a) plan (b) cross-section (b) bearing #1 (c) bearing #2

Figure 6. MCNP absorbed dose rates of the rubber layers, Type B LDR bearings

6. IRRADIATION AND PRE- AND POST-IRRADITION MECHNICAL TESTING

Type A LDR and LR bearings

Two Type A LDR and LR bearings were irradiated to cumulative absorbed doses of 25, 100, and 200 kGy, with mechanical testing performed after each irradiation in the SBTM at the University at Buffalo. The irradiation details are presented in Tables 1 and 2. One LDR and one LR bearing were rotated four times, each for a quarter of the total exposure time, to try to achieve a *uniform* dose to the perimeter of the bearing and to study the impact of the dose gradient on the mechanical properties of the bearings, if any.

Table 3 summarizes the mechanical testing protocols for the Type A LDR and LR bearings. An axial load of 62 kN was applied, generating approximately 3.5 MPa axial pressure, to simulate gravity. The test motion consisted of the four cycles of a triangular displacement series. The bearings were tested at frequencies of 0.01 and 1 Hz to study their velocity-dependent behavior, if any. The bearings were tested at peak shear strains of 25%, 50%, 75%, and 100%. In this paper, results for the 50% and 100% shear strain tests at a frequency of 1 Hz, are presented.

Table 1. Irradiation details of the Type A LDR bearings

Item	Rotated	Target dose, kGy	Irradiation start date	Exposure time, min	Dose rate*, Gy/min	Achieved dose, kGy	Cumulative absorbed dose, kGy
Round 1							
LDR-A1	No	25	4/22/2024	540	44	24	24
LDR-A2	Yes	25	4/22/2024	540	44	24	24
Round 2							
LDR-A1	No	75	8/29/2024	1,920	42	81	105
LDR-A2	Yes	75	9/4/2024	1,920	42	81	105
Round 3							
LDR-A1	No	100	11/4/2024	2,820	41	116	221
LDR-A2	Yes	100	11/6/2024	2,820	41	116	221

*Corrected for the decay of ^{60}Co to the irradiation start date

Table 2. Irradiation details of the Type A LR bearings

Item	Rotated	Target dose, kGy	Irradiation start date	Exposure time, min	Dose rate, Gy/min	Achieved dose, kGy	Cumulative absorbed dose, kGy
Round 1							
LR-A1	No	25	4/22/2024	540	43	23	23
LR-A2	Yes	25	4/22/2024	540	43	23	23
Round 2							
LR-A1	No	75	9/13/2024	1,920	40	78	101
LR-A2	Yes	75	9/11/2024	1,920	40	78	101
Round 3							
LR-A1	No	100	11/10/2024	2,820	40	112	212
LR-A2	Yes	100	11/8/2024	2,820	40	112	212

Table 3. Mechanical testing program for the Type A LDR and LR bearings

Test	No. of cycles	Axial load, kN	Frequency, Hz	Displacement amplitude, mm, [%]*
TA-1	4	62	0.01	15 [25]
TA-2	4	62	1	15 [25]
TA-3	4	62	0.01	30 [50]
TA-4	4	62	1	30 [50]
TA-5	4	62	0.01	45 [75]
TA-6	4	62	1	45 [75]
TA-7	4	62	0.01	60 [100]
TA-8	4	62	1	60 [100]

*Peak shear strain = peak displacement divided by the total thickness of rubber

Figure 7 enables a comparison of the horizontal force-displacement hysteresis, pre- and post-irradiation, for the LDR-A1 and LR-A1 bearings and test TA-8. No significant change is observed in their mechanical properties. Figures 8 and 9 illustrate the change in mechanical properties as a function of cumulative absorbed gamma dose. The percentage change in the mechanical properties is small, and less than 20%. No effect on mechanical properties due to rotation of the isolators in the irradiator was observed. There were no signs of debonding of the elastomer from the steel shims at an absorbed dose of 200 kGy.

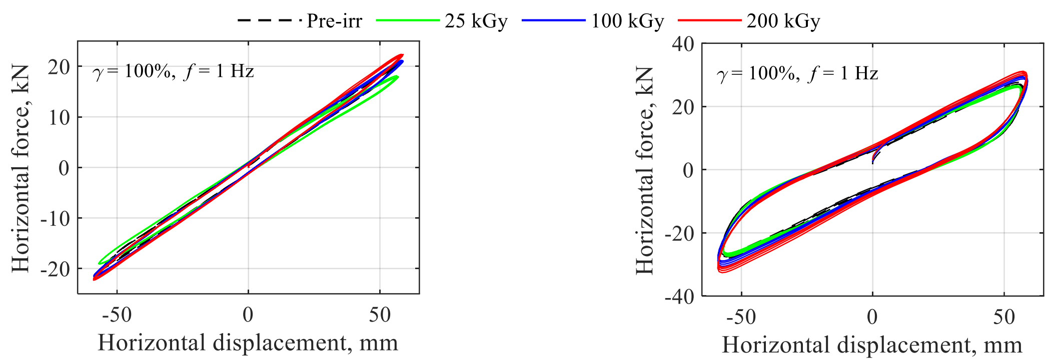

(a) LDR-A1, test TA-8 (b) LR-A1, test TA-8

Figure 7. Pre- and post-irradiation hysteretic response, Type A bearings

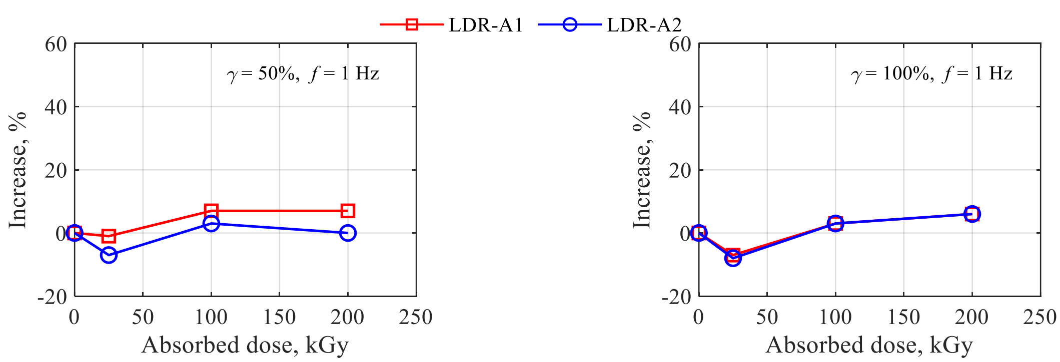

(a) test TA-4 (b) test TA-8

Figure 8. Change in shear modulus, Type A LDR bearings, as a function of cumulative absorbed gamma dose

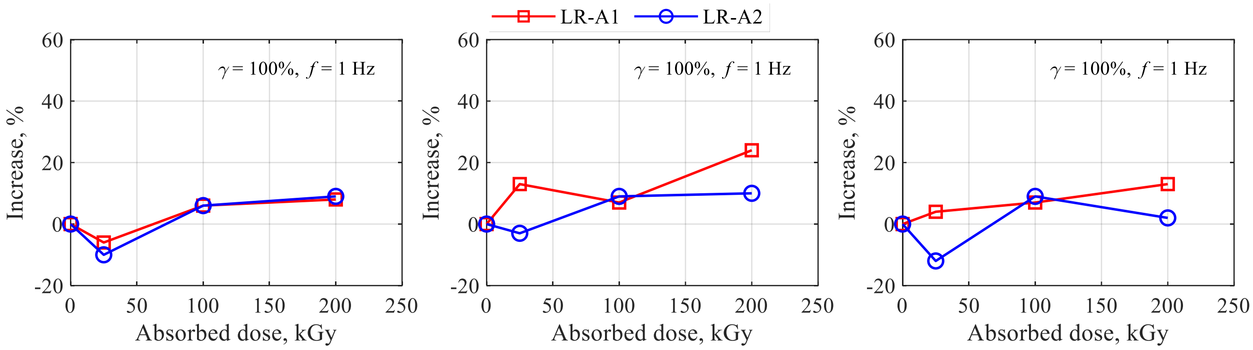

(a) shear modulus (b) characteristic strength (c) energy dissipation per cycle

Figure 9. Change in mechanical properties, Type A LR bearing, as a function of cumulative absorbed gamma dose for test TA-8

Type B LDR bearings

Four Type B LDR bearings were irradiated to cumulative absorbed doses of 25, 100, and 200 kGy, followed by mechanical testing after each irradiation. Table 4 presents irradiation details of the Type B LDR bearings. Two bearings were stacked, as shown in Figure 6b, for irradiation. One stack of two bearings was rotated.

The testing protocols for Type B LDR bearings were the same as those for the Type A LDR bearings, as presented in Table 3, except for the axial load and peak displacements. An axial load of 22 kN was imposed, and displacements corresponding to peak shear strains of 25%, 50%, 75%, and 100% were applied: 8, 16, 24, and 32 mm, respectively. The test motions for the Type B bearings are denoted as TB-1 to TB-8, replacing A with B in Table 3.

Table 4. Irradiation details of the Type B LDR bearings

Item	Location in stack	Rotated	Target dose, kGy	Irradiation start date	Exposure time, min	Dose rate, Gy/min	Achieved dose, kGy	Cumulative absorbed dose, kGy
Round 1								
LDR-B1	Top	No	25	9/15/2024	462	48	22	22
LDR-B3	Bottom	No	25	9/15/2024	462	54	25	25
LDR-B4	Top	Yes	25	9/17/2024	462	48	22	22
LDR-B2	Bottom	Yes	25	9/17/2024	462	54	25	25
Round 2								
LDR-B1	Top	No	75	11/13/2024	1,410	47	67	89
LDR-B3	Bottom	No	75	11/13/2024	1,410	53	75	100
LDR-B4	Top	Yes	75	11/14/2024	1,410	47	67	89
LDR-B2	Bottom	Yes	75	11/14/2024	1,410	53	75	100
Round 3								
LDR-B1	Top	No	100	1/2/2025	1,920	46	89	178
LDR-B3	Bottom	No	100	1/2/2025	1,920	52	100	200
LDR-B4	Top	Yes	100	1/4/2025	1,920	46	89	178
LDR-B2	Bottom	Yes	100	1/4/2025	1,920	52	100	200

Figures 10a and 10b enable a comparison of the force-displacement hysteresis, pre- and post-irradiation, for the LDR-B1 bearing for tests TB-4 and TB-8, respectively. The results show an increase in the stiffness of the bearings with an increase in the absorbed dose. Figures 11a and 11b illustrate the change in the shear modulus of the rubber as a function of cumulative absorbed gamma dose for tests TB-4 and TB-8, respectively. The shear modulus increases with increasing absorbed gamma dose: a 10%, 25%, and 40% increase at absorbed doses of 25, 100, and 200 kGy, respectively for LDR-B1. No signs of debonding of the elastomer from the steel shims were observed.

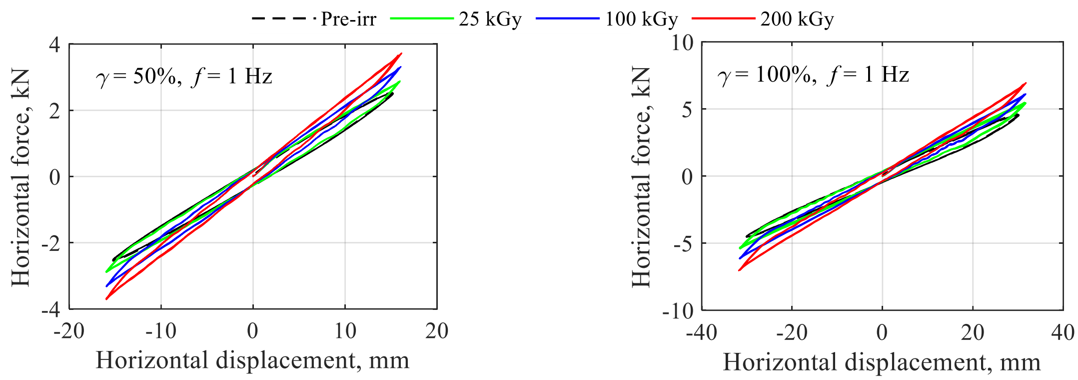

(a) LDR-B1, test TB-4 (b) LDR-B1, test TB-8

Figure 10. Pre- and post-irradiation hysteretic behavior, LDR-B1

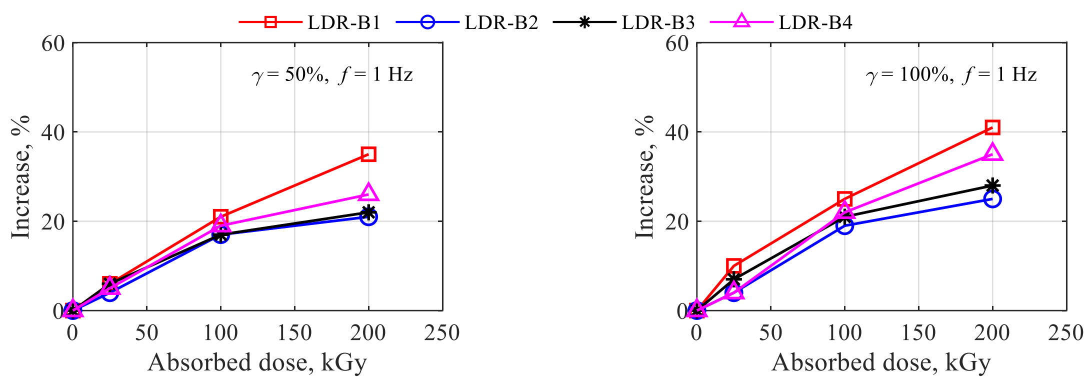

(a) test TB-4 (b) test TB-8

Figure 11. Change in shear modulus of rubber, Type B LDR bearings, as a function of cumulative absorbed gamma dose

7. SUMMARY AND FUTURE WORK

This paper presents the results of interdisciplinary research on the effect of gamma radiation on the mechanical performance of seismic protective devices, involving experiments at UB and INL. The seismic protective devices were irradiated at INL using an FTS irradiator and mechanically tested at UB. A model of the FTS irradiator was developed in MCNP and validated using Fricke dosimetry. The MCNP model was used to determine the exposure time in the FTS irradiator required to achieve a target absorbed dose in the LDR and LR bearings. Pre- and post-irradiation mechanical testing results for LDR and LR bearings are presented, characterizing changes in their mechanical properties as a function of cumulative absorbed gamma dose. The mechanical properties of the Type A LDR and LR bearings were not affected by gamma radiation for an average absorbed dose of 200 kGy. The stiffness of the Type B LDR bearings increased with the absorbed dose. There was no evidence of debonding of the rubber layers from the steel shims, indicating failure of the adhesive, in any of the tests performed to date.

Near-term work will involve the irradiation and mechanical testing of SFT and TFP isolators, GERB viscoelastic dampers, and coil-spring isolators, and the continued irradiation of the LDR and LR bearings described in this paper. Raman spectroscopy will be performed on rubber samples from the Type B LDR bearings to analyze changes in microstructure due to gamma exposure. Longer-term efforts will include MCNP simulations of prototype seismic protective devices and their installation near reactor vessels to guide decision making by reactor developers, together with revisions to numerical models of isolators and dampers in commercial structural analysis software to account for the effects of gamma radiation.

8. ACKNOWLEDGMENTS

The authors thank the U.S. Department of Energy for supporting the research project under Contract DE-AC07 051D14517 as a part of Nuclear Science User Facility Agreement No. 22-27129 and for enabling access to the Sawtooth High-Performance Computing Facility at INL, and Dynamic Isolation Systems for providing the LDR and LR bearings at no cost to the project.

9. REFERENCES

Detwiler, R. S., McConn, R. J., Grimes, T. F., Upton, S. A., and Engel, E. J. (2021). "Compendium of material composition data for radiation transport modeling." *LA-UR-22-30006*, Pacific Northwest National Laboratory (PNNL), Richland, WA.

Fricke, H., Hart, E. J., and Smith, H. P. (1938). "Chemical reactions of organic compounds with X-ray activated water." *The Journal of Chemical Physics*, 6(5), 229-240.

Lal, K. M., Parsi, S. S., Kosbab, B. D., Ingersoll, E. D., Charkas, H., and Whittaker, A. S. (2022). "Towards standardized nuclear reactors: Seismic isolation and the cost impact of the earthquake load case." *Nuclear Engineering and Design*, 386, 111487.

Mir, F. U. H., Whittaker, A. S., Kosbab, B. D., and Nguyen, N. (2023). "Characterizing the seismic response of a molten salt nuclear reactor." *Earthquake Engineering & Structural Dynamics*, 52(7), 2025-2046.

Patel, A. D., Peterman, D. R., and Kitcher, E. D. (2024a). "Benchmarking MCNP models to support gamma irradiation experiments." *Transactions: 2024 ANS Winter Conference and Expo*, November 17-21, Orlando, FL, 612-615.

Patel, A. D., Peterman, D. R., Kitcher, E. D., Bolisetti, C., and Whittaker, A. S. (2024b). "Influence of gamma radiation on the mechanical behavior of seismic protective devices." *Proceedings: 2024 International Congress on Advances in Nuclear Power Plants (ICAPP)*, June 16-19, Las Vegas, NV, 42-52.

Patel, A. D., Peterman, D. R., Kitcher, E. D., Bolisetti, C., and Whittaker, A. S. (2025a). "Modeling radiation effects of the mechanical properties of the 3D viscoelastic dampers for seismic isolation." *Transactions: 2025 ANS Winter Conference and Expo*, November 9–12, Washington, DC.

Patel, A. D., Peterman, D. R., Kitcher, E. D., Bolisetti, C., and Whittaker, A. S. (2025b). "Effects of gamma radiation on the mechanical properties of spherical sliding and coil-spring isolators." *Proceedings: 19th World Conference on Seismic Isolation, Energy Dissipation and Active Vibration Control of Structures (19WCSI)*, September 15-19, Berkeley, CA.

Patel, A. D., Peterman, D. R., Kitcher, E. D., Bolisetti, C., and Whittaker, A. S. (2025c). "Integrating HPC simulations and physical experiments to characterize the effects of gamma radiation on seismic protective devices." *Nuclear Engineering and Design*.

Yu, C.-C., Bolisetti, C., Coleman, J. L., Kosbab, B., and Whittaker, A. S. (2018). "Using seismic isolation to reduce risk and capital cost of safety-related nuclear structures." *Nuclear Engineering and Design*, 326, 268-284.